High Data Rate Discrete-Cosine-Spreading Aided *M*-Ary Differential Chaos Shift Keying Scheme With Low PAPR

Zuwei Chen[®], Lin Zhang[®], Member, IEEE, and Zhiqiang Wu[®], Senior Member, IEEE

Abstract—Traditional differential chaos shift keying (DCSK) systems have low spectrum efficiency since half of time slots are used to transmit the reference chaotic signals. Our objective is to utilize the orthogonality of chaotic vectors and orthogonal cosine functions to construct a high data rate M-ary modulation scheme while providing improved reliability over wireless channels. In this brief, we propose a discrete-cosine-spreading (DCS) aided M-ary DCSK scheme. In our design, we first utilize the Gram-Schmidt algorithm to generate orthogonal chaotic basis vectors, then the linear combination of these vectors is used for M-ary modulations to improve the data rate. In order to suppress the interferences between modulated signals and reduce the peak to average power ratio (PAPR) induced by the overlapping of linear combinations, subsequently we apply discrete cosine codes to spread the modulated symbols. The resultant symbols are respectively transmitted over the quadrature and inphase channels. Furthermore, we derive the theoretical bit error rate (BER) expression over additive white Gaussian noise (AWGN) channel and multipath Rayleigh channels, then we analyze the computational complexity. Simulation results validate the theoretical derivations, and demonstrate that compared with the benchmark schemes, the proposed scheme could achieve higher data rate with the improved bandwidth efficiency, better BER performances over multipath fading channels, and lower PAPR.

Index Terms—Differential chaos shift keying (DCSK), Discrete cosine spreading (DCS), Gram-Schmidt transform, orthogonal basis, reliability.

Manuscript received January 28, 2020; revised March 8, 2020; accepted March 10, 2020. Date of publication March 13, 2020; date of current version November 4, 2020. This work was supported in part by the open research fund from Shandong Provincial Key Laboratory of Wireless Communication Technologies under Grant SDKLWCT-2019-05, in part by the State's Key Project of Research and Development Plan under Grant 2017YFE0121300-6, in part by the NSF under Grant 1748494, in part by the Key Research & Development and Transformation Plan of Science and Technology Program for Tibet Autonomous Region under Grant XZ201901-GB-16, in part by the Special fund for the development of local universities supported by the Central Finance of Tibet University in 2018, and in part by the Project of National Natural Science Foundation of China under Grant 61602531. This brief was recommended by Associate Editor Y. Xia. (Corresponding author: Lin Zhang.)

Zuwei Chen is with the School of Electronic and Information Technology, Sun Yat-sen University, Guangzhou 510006, China (e-mail: chenzw25@mail2.sysu.edu.cn).

Lin Zhang is with the School of Electronic and Information Technology, Sun Yat-sen University, Guangzhou 510006, China, and also with the Shandong Provincial Key Laboratory of Wireless Communication Technologies, Jinan 250100, China (e-mail: isszl@mail.sysu.edu.cn).

Zhiqiang Wu is with the Department of Electrical Engineering, Tibet University, Lhasa 850012, China, and also with the Department of Electrical Engineering, Wright State University, Dayton, OH 45435 USA (e-mail: zhiqiang.wu@wright.edu).

Color versions of one or more of the figures in this article are available online at http://ieeexplore.ieee.org.

Digital Object Identifier 10.1109/TCSII.2020.2980738

I. INTRODUCTION

In THE past two decades, chaotic communications have attracted lots of research interests thanks to the antijamming capabilities and high security performances achieved by chaotic transmissions. Compared with the coherent chaotic modulation, the non-coherent chaotic modulation such as the differential chaos shift keying (DCSK) has received more attentions in recent years, since no complex chaotic synchronization circuit is required at receivers and thus the practicability is enhanced.

The major drawback of the DCSK scheme is the low spectrum efficiency due to the transmission of the reference chaotic signal using half of time slots. In order to improve the spectrum efficiency, many research works have been done. Reference [1] proposed a code-shifted differential chaos shift keying (CS-DCSK) scheme, which transmitted the reference signal and the information bearing signals modulated by Walsh codes in the same time slot. Later on, the idea of exploiting Walsh codes to transmit the chaotical modulated signals was extended and a generalized code-shifted differential chaos shift keying (GCS-DCSK) scheme was proposed by [2]. Furthermore, [3] proposed a multilevel code-shifted differential chaos shift keying (MCS-DCSK) [3] scheme to improve the data rate.

Based on these achievements, *M*-ary modulation schemes were proposed to further improve the GCS-DCSK scheme [4] and the MCS-DCSK scheme [5]. In addition, Hilbert transformation was utilized by [6] to propose a quadrature chaos shift keying (QCSK) scheme to achieve twice data rate, and [7] used Hilbert transformation and Walsh codes to achieve higher data rate and in [8], the authors used the Gram-Schmidt algorithm to generate multiple orthogonal chaos signals to transmit the information to attain higher data rate. Expect for the orthogonality of pseudo random codes, the orthogonality in the frequency domain was also exploited to improve the spectrum efficiency, such as the orthogonal frequency division multiplexing (OFDM)-based OCVSK scheme [9] and multi-carrier chaos shift keying (MC-CSK) [10].

However, these *M*-ary high order DCSK modulation schemes using Walsh codes have weak resistances to the multipath fading, thereby leading to degraded performances. Besides, the summation operations contained in *M*-ary modulation may induce the issue of larger peak to average power ratio (PAPR). Moreover, the traditional *M*-ary modulation schemes require the order of the Walsh code to be the *n*-th power of two, thus the flexibility and the practicality is constrained.

1549-7747 © 2020 IEEE. Personal use is permitted, but republication/redistribution requires IEEE permission. See https://www.ieee.org/publications/rights/index.html for more information.

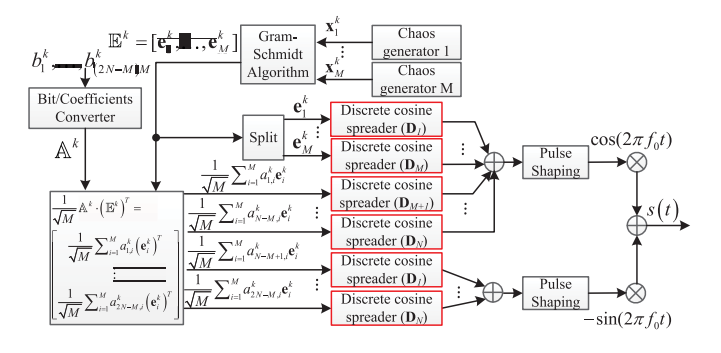


Fig. 1. The DCS-aided M-ary DCSK transmitter.

Different from the existing high data rate chaotic modulation schemes based on Walsh codes, in this brief, we propose a discrete-cosine-spreading (DCS) aided *M*-ary DCSK scheme to modulate the user data with multiple orthogonal chaotic basis vectors and the discrete cosine functions, thus the reliability performance are improved while providing high data rate transmissions.

In our design, at the transmitter, the chaotic signals generated by the chaos generator are firstly transformed by the Gram-Schmidt algorithm to construct multiple orthogonal basis vectors for achieving *M*-ary modulations of user data. Subsequently, the information-bearing chaotic modulated signals are spread by the orthogonal discrete cosine transform (DCT) matrix, whose dimension can be arbitrary positive integer, to enlarge the Euclidean distances and reduce the PAPR. The resultant signals are then transmitted over channels. At the receiver, the reverse operations are performed to recover the estimates of the received signals.

Briefly, the main contributions include:

- We propose to utilize the discrete cosine codes to spread the information-bearing chaotical modulated signals to achieve higher data rate with enhanced reliability over multipath channels and lower PAPR.
- The proposed DCS-M-DCSK scheme achieves better practicality than counterpart schemes, since the DCS codes can have the order of the arbitrary positive integer.
- Theoretical BER performances of the proposed design are analyzed over the additive white Gaussian noise (AWGN) channel and multipath Rayleigh fading channels.

The remainder of this brief is organized as follows. The system model of DCS-M-DCSK is presented in Section II. Then we analyze the theoretical BER performances and the computational complexity in Section III. Section IV provides simulation results and Section V concludes this brief.

II. SYSTEM MODEL

In this section, the transmitter and receiver architectures of DCS-M-DCSK system are presented.

A. Transmitter

At the transmitter shown in Fig. 1, in the k-th symbol duration, M chaos generators generate M different chaotic sequences, denoted by $\mathbf{x}_1^k, \ldots, \mathbf{x}_M^k$ respectively. Let $\mathbf{x}_i^k = (x_{i,0}^k, x_{i,1}^k, \ldots, x_{i,\beta-1}^k)^T$ denotes the i-th sequence, where β is the sequence length. Then the Gram-Schmidt algorithm is applied to orthogonalize $\mathbf{x}_1^k, \ldots, \mathbf{x}_M^k$ to produce multiple orthogonal chaotic basis vectors to modulate the user data. Then the discrete cosine spreading is performed to lower the

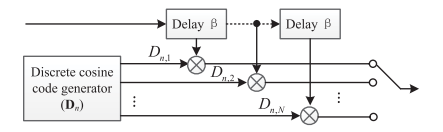


Fig. 2. The discrete cosine spreader structure.

PAPR and enhance the reliability performances. More details are given as follows.

1) *M-Ary Modulation:* Applying the Gram-Schmidt algorithm [11], we generate M orthogonal chaotic basis vectors, denoted by $\mathbf{e}_1^k, \dots, \mathbf{e}_M^k$, from $\mathbf{x}_1^k, \dots, \mathbf{x}_M^k$ by

$$\mathbf{e}_{i}^{k} = \begin{cases} \frac{\mathbf{x}_{1}^{k}}{\sqrt{\langle \mathbf{x}_{1}^{k}, \mathbf{x}_{1}^{k} \rangle}}, & i = 1\\ \frac{\mathbf{x}_{i}^{k} - \sum_{n=1}^{i-1} \langle \mathbf{x}_{i}^{k}, \mathbf{e}_{n}^{k} \rangle \mathbf{e}_{n}^{k}}{\sqrt{\left\langle \mathbf{x}_{i}^{k} - \sum_{n=1}^{i-1} \langle \mathbf{x}_{i}^{k}, \mathbf{e}_{n}^{k} \rangle \mathbf{e}_{n}^{k}, \mathbf{x}_{i}^{k} - \sum_{n=1}^{i-1} \langle \mathbf{x}_{i}^{k}, \mathbf{e}_{n}^{k} \rangle \mathbf{e}_{n}^{k} \rangle}}, & i = 2, \dots, M \end{cases}$$
(1)

where $\langle \mathbf{x}_i^k, \mathbf{e}_n^k \rangle$ represents the inner product of vector \mathbf{x}_i^k and \mathbf{e}_n^k , which is calculated by $\langle \mathbf{x}_i^k, \mathbf{e}_n^k \rangle = \sum_{j=0}^{\beta-1} x_{i,j}^k e_{n,j}^k$ and j represents the index of chips of the specific vector. These basis vectors constitutes a matrix $\mathbb{E}^k (= [\mathbf{e}_1^k, \dots, \mathbf{e}_M^k])$ to be used as the reference vectors.

On the other hand, the serially input user data bits $b_1^k,\ldots,b_{(2N-M)M}^k$ are mapped to a coefficient matrix \mathbb{A}^k , wherein the element is denoted by $a_{v,i}^k \in \{1,-1\}(v=1,\ldots,2N-M)(i=1,\ldots,M)$. Subsequently, we modulate \mathbb{A}^k with the normalized reference chaotic matrix $\frac{1}{\sqrt{M}}(\mathbb{E}^k)^T$, and the information-bearing vector is denoted by $\frac{1}{\sqrt{M}}\sum_{i=1}^M a_{v,i}^k \mathbf{e}_i^k$.

2) Discrete Cosine Spreading: Next, we propose to spread both the reference and information bearing vectors by DCS codes. As shown in Fig. 2, let \mathbf{D}_n represent the *n*-th row of the matrix with the element $D_{n,m}$ (n = 1, ..., N) (m = 0, ..., N-1) defined as [12]

$$D_{n,m} = \begin{cases} \sqrt{\frac{1}{N}} \cos\left(\frac{(2m+1)(n-1)\pi}{2N}\right), & n = 1\\ \sqrt{\frac{2}{N}} \cos\left(\frac{(2m+1)(n-1)\pi}{2N}\right), & n = 2, \dots, N \end{cases}$$
 (2)

where N could have arbitrarily integer value. Let SF denote the spreading factor, then $SF = N\beta$. It is worth mentioning that although Walsh codes can also be applied to spread signals, the dimension is 2^n [3] since they are constructed by the row or column of the Hadamard matrix recursively. Thus the practicality is worse than the discrete cosine codes.

Notably, DCS codes are orthogonal and satisfy $\sum_{m=0}^{N-1} D_{n,m} D_{k,m} = 0$ $(n \neq k)$ [13]. In addition, in order to keep the transmitting energy as a constant, they are normalized to $\sum_{m=0}^{N-1} D_{n,m}^2 = 1$ [12].

Then after the pulse shaping represented by $f_T(t-jT_c)$, wherein T_c is the duration time, we obtain the transmitted signal in the k-th symbol duration as

$$s(t) = \left(\sum_{i=1}^{M} \sum_{m=0}^{N-1} D_{i,m} e_i^k(t - mT_c) + \frac{1}{\sqrt{M}} \sum_{\nu=1}^{N-M} \sum_{i=1}^{M} \sum_{m=0}^{N-1} a_{\nu,i}^k D_{\nu+M,m} e_i^k(t - mT_c) \right) \cos(2\pi f_0 t) - \frac{1}{\sqrt{M}} \sum_{\nu=1}^{N} \sum_{i=1}^{M} \sum_{m=0}^{N-1} a_{\nu+N-M,i}^k D_{\nu,m} e_i^k(t - mT_c) \sin(2\pi f_0 t)$$
(3)

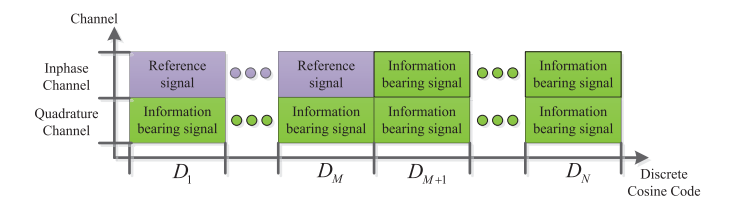


Fig. 3. The signal transmission over the inphase channel and the quadrature channel.

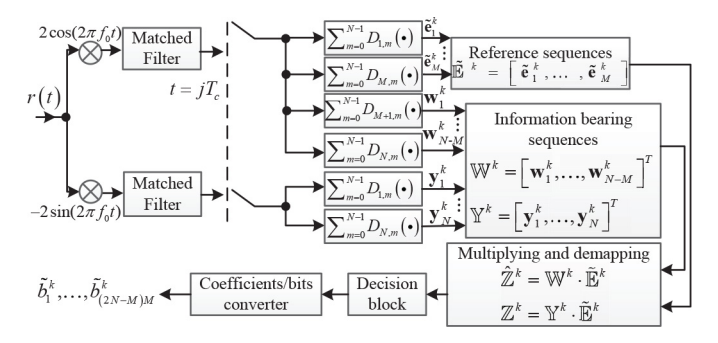


Fig. 4. The DCS-aided M-ary DCSK receiver.

Subsequently, s(t) is transmitted over channels. As illustrated by Fig. 3, M reference symbols and N-M information bearing symbols are transmitted via the inphase channel, while N information bearing symbols are transmitted over the quadrature channel.

B. Receiver

At the DCS-aided M-ary DCSK receiver, reverse operations are performed. In the AWGN channel, the received signal r(t)can be represented by

$$r(t) = s(t) + n(t) \tag{4}$$

where n(t) denotes the Gaussian noise having the zero mean and power spectral density of $N_0/2$.

As shown in Fig. 4, after matched filtering and sampling, the received signal is correlated with each DCS code to recover the reference chaotic vectors and data bearing vectors. More explicitly, let $\tilde{\mathbf{e}}_{u}^{k} = (\tilde{e}_{u,0}^{k}, \tilde{e}_{u,1}^{k}, \dots, \tilde{e}_{u,\beta-1}^{k})^{T}$ $(u = 1, \dots, M)$ denote the *u*-th recovered reference vector, then the *j*-th chip

$$\tilde{e}_{u,j}^{k} = \sum_{m=0}^{N-1} \left(\sum_{i=1}^{M} D_{i,m} e_{i,j}^{k} + \frac{1}{\sqrt{M}} \sum_{v=1}^{N-M} \sum_{i=1}^{M} a_{v,i}^{k} D_{v+M,m} e_{i,j}^{k} \right) D_{u,m} + \sum_{m=0}^{N-1} n_{I,j}^{k} D_{u,m} = e_{u,j}^{k} + \sum_{m=0}^{N-1} n_{I,j}^{k} D_{u,m}$$
(5)

where $n_{I,j}^k$ is the noise received from the in-phase channel. Besides, let $\mathbf{y}_g^k = (y_{g,0}^k, y_{g,1}^k, \dots, y_{g,\beta-1}^k)^T$ $(g = 1, \dots, N)$ denote the recovered information bearing vector over the quadrature channel, then the *j*-th chip is calculated by

$$y_{g,j}^{k} = \sum_{m=0}^{N-1} \left(\frac{1}{\sqrt{M}} \sum_{\nu=1}^{N} \sum_{i=1}^{M} a_{\nu+N-M,i}^{k} D_{\nu,m} e_{i,j}^{k} + n_{Q,j}^{k} \right) D_{g,m}$$

$$= \frac{1}{\sqrt{M}} \sum_{i=1}^{M} a_{g+N-M,i}^{k} e_{i,j}^{k} + \sum_{m=0}^{N-1} n_{Q,j}^{k} D_{g,m}$$
(6)

where $n_{Q,j}^k$ is the noise received from the quadrature channel while for the inphase channel, the j-th chip of \mathbf{w}_g^k (g =

$$1, \ldots, N-M$$
) is

$$w_{g,j}^{k} = \frac{1}{\sqrt{M}} \sum_{i=1}^{M} a_{g,i}^{k} e_{i,j}^{k} + \sum_{m=0}^{N-1} n_{I,j}^{k} D_{g+M,m}$$
 (7)

Subsequently, the chaotic demodulation is performed with the reference chaotic matrix $\tilde{\mathbb{E}}^k$ and the information-bearing matrix \mathbb{Y}^k . As shown in Fig. 4, the resultant decision matrix is $\hat{\mathbb{Z}}^k = \mathbb{W}^k \cdot \tilde{\mathbb{E}}^k$ and $\mathbb{Z}^k = \mathbb{Y}^k \cdot \tilde{\mathbb{E}}^k$, wherein the element, i.e., the decision variable $\hat{z}_{g,u}^k$ and $z_{g,u}^k$ are expressed as

$$\hat{z}_{g,u}^{k} = \sum_{j=0}^{\beta-1} w_{g,j}^{k} \tilde{e}_{u,j}^{k} \qquad z_{g,u}^{k} = \sum_{j=0}^{\beta-1} y_{g,j}^{k} \tilde{e}_{u,j}^{k}$$
 (8)

At last, we demodulate $\hat{z}_{g,u}^k$ and $z_{g,u}^k$ to obtain the estimates denoted by $\tilde{b}_1^k, \ldots, \tilde{b}_{(2N-M)M}^k$.

III. PERFORMANCE ANALYSIS

In this section, we analyze the BER, PAPR performances and the computational complexity for the proposed design.

A. BER Analysis

Considering that $\sum_{j=0}^{\beta-1} e_{i,j}^k e_{u,j}^k = 0, i \neq u$ and substituting Eq. (5) and Eq. (7) into Eq. (8), we can calculate the decision variable by

$$\hat{z}_{g,u}^{k} = \sum_{j=0}^{\beta-1} \left(\frac{1}{\sqrt{M}} \sum_{i=1}^{M} a_{g,i}^{k} e_{i,j}^{k} + \sum_{m=0}^{N-1} n_{I,j}^{k} D_{g+M,m} \right)$$

$$\times \left(e_{u,j}^{k} + \sum_{m=0}^{N-1} n_{I,j}^{k} D_{u,m} \right)$$

$$= \frac{1}{\sqrt{M}} \sum_{j=0}^{\beta-1} a_{g,u}^{k} \left(e_{u,j}^{k} \right)^{2} + \frac{1}{\sqrt{M}} \sum_{m=0}^{N-1} \sum_{i=1}^{M} \sum_{j=0}^{\beta-1} a_{g,i}^{k} e_{i,j}^{k} n_{I,j}^{k} D_{u,m}$$

$$+ \sum_{m=0}^{N-1} \sum_{j=0}^{\beta-1} n_{I,j}^{k} D_{g+M,m} e_{u,j}^{k} + \underbrace{\frac{1}{\sqrt{M}} \sum_{i=1, i \neq u}^{M} \sum_{j=0}^{\beta-1} a_{g,i}^{k} e_{i,j}^{k} e_{u,j}^{k}}_{=0} }_{=0}$$

$$+ \sum_{j=0}^{\beta-1} \left(\sum_{m=0}^{N-1} n_{I,j}^{k} D_{g+M,m} \right) \left(\sum_{m=0}^{N-1} n_{I,j}^{k} D_{u,m} \right)$$

$$(9)$$

Substituting Eq. (5) and Eq. (6) into Eq. (8), we can get $\hat{z}_{g,u}^k$ and since the decision variables $\hat{z}_{g,u}^k$ and $z_{g,u}^k$ have the same statistical characteristics, we only need to evaluate the numerical characteristics for one of them. On the condition that $a_{g,i}^k=1$ and $\sum_{m=0}^{N-1}D_{n,m}^2=1$, we can derive that

$$E\left[\hat{z}_{g,u}^{k}\right] = \frac{1}{\sqrt{M}}\beta E\left[\left(e_{u,j}^{k}\right)^{2}\right] = \frac{(2N - M)ME_{b}}{2N\sqrt{M}}$$

$$\operatorname{var}\left[\hat{z}_{g,u}^{k}\right] = \frac{N_{0}\beta E\left[\left(e_{u,j}^{k}\right)^{2}\right]}{2} + \frac{MN_{0}\beta E\left[\left(e_{i,j}^{k}\right)^{2}\right]}{2M} + \frac{\beta N_{0}^{2}}{4}$$

$$= \frac{(2N - M)ME_{b}N_{0}}{2N} + \frac{\beta N_{0}^{2}}{4} \tag{10}$$

where $E[\cdot]$ and $var[\cdot]$ respectively represent the numerical expectation and the variance of a specific random variable, E_b is the bit energy expressed by $E_b = \frac{2N\beta \mathrm{E}[(e_b^k)^2]}{(2N-M)M}$

Scheme	Date Rate K	Bandwidth efficiency
DCS-M-DCSK	M(2N-M)	M(2N-M)/(SF)
OM-DCSK [7] OCVSK [8] MCS-DCSK [3] MCS-MDCSK [5] MC-CSK [10]	$\begin{array}{c} log_2(2N) \\ M \\ P \\ (P)log_2(M)/2 \\ Nlog_2(N) \end{array}$	$log_2(2N)/(SF)$ M/(SF) P/(SF) $(P)log_2(M)/(2SF)$ $Nlog_2(N)/(SF)$

Then we could obtain the BER expression over AWGN channel as

$$P_e^{AWGN} = \frac{1}{2}erfc\left[\frac{E\left[\hat{z}_{g,u}^k\right]}{\sqrt{2var\left[\hat{z}_{g,u}^k\right]}}\right]$$
$$= \frac{1}{2}erfc\left[\left(\frac{4NN_0}{(2N-M)E_b} + \frac{2N^2\beta N_0^2}{(2N-M)^2ME_b^2}\right)^{-\frac{1}{2}}\right] (11)$$

where $erfc(x) = \frac{2}{\sqrt{\pi}} \int_{x}^{\infty} e^{-t^2} dt$ is the complementary error function.

Moreover, for the multipath fading channel containing L independent and identically-distributed (i.i.d) paths with the gain of $\alpha_l(l=1,2,\ldots,L)$, the instantaneous signal to noise ratio (SNR) γ_b is $\gamma_b = \sum_{l=1}^L \alpha_l^2 \frac{E_b}{N_0}$ with $\mathrm{E}(\alpha_l^2) = \frac{1}{L}$. For Rayleigh fading channels, the probability density function of γ_b is $f(\gamma_b) = \frac{\gamma_b^{L-1}}{\bar{\gamma}^L(L-1)!} \exp^{-\frac{\gamma_b}{\bar{\gamma}}}$, where $\bar{\gamma}$ denotes the average bit-SNR per path given by $\bar{\gamma} = \frac{1}{L} \frac{E_b}{N_0}$. Thus we can obtain the conditional BER as [3]

$$P_e(\gamma_b) = \frac{1}{2} erfc \left[\left(\frac{4N}{(2N-M)\gamma_b} + \frac{2N^2\beta}{(2N-M)^2M\gamma_b^2} \right)^{-\frac{1}{2}} \right]$$
(12)

Then we can derive the BER expression of DCS-M-DCSK system over multipath Rayleigh fading channel as

$$P_e^{MULTIPATH} = \int_0^{+\infty} P_e(\gamma_b) f(\gamma_b) d\gamma_b. \tag{13}$$

B. Date Rate and Complexity Analysis

Table I compares the data rate denoted by K and the bandwidth efficiency of the proposed scheme and counterpart schemes, wherein SF respresents the spreading factor. Notably, for OCVSK [8], $SF = 2\beta$ but for other schemes, $SF = N\beta$. In addition, for OM-DCSK [7], MCS-DCSK [3] and MCS-MDCSK [5], N is the order of the Walsh codes and P ($P \le N - 2$) is the number of Walsh codes used for information delivery, while for MC-CSK [10], N represents the number of subcarriers. Moreover, for OCVSK [8], M equals to the number of orthogonal basis vectors, while for MCS-MDCSK, M is the modulation order.

Furthermore, it can be noticed that the DCS-M-DCSK scheme achieves higher data rate and efficiency than benchmark schemes. For example, when N=8 and M=4, the proposed DCS-M-DCSK system achieves the data rate of 48 bits/symbol and the bandwidth efficiency of $\frac{48}{SF}$, while the maximum data rate of the MCS-DCSK and MCS-MDCSK schemes is 6 bits/symbol and the bandwidth efficiency is $\frac{6}{SF}$. In addition, the data rate of OM-DCSK, OCVSK, MC-CSK

TABLE II
COMPUTATIONAL COMPLEXITY COMPARISONS

Data rate K	Scheme	Addition operations	Multiplication operations
48 bits/symbol	$\begin{array}{l} {\rm DCS\text{-}}M\text{-}{\rm DCSK}(N=8,M=4)\\ {\rm OM\text{-}}{\rm DCSK}~[7](N=2^{47})\\ {\rm OCVSK}~[8](M=48)\\ {\rm MCS\text{-}}{\rm DCSK}~[3](N=64,P=48)\\ {\rm MCS\text{-}}{\rm DCSK}~[5](N=64,P=48,M=4) \end{array}$	$\begin{array}{c} 73SF - 58 \\ (2^{49} + 1 - \frac{1}{2^{47}})SF - 2^{48} \\ 2352SF - 2401 \\ 96.984375SF - 48 \\ 96.984375SF - 48 \end{array}$	$\begin{array}{c} 88SF \\ 3(2^{48}+1)SF \\ 2352.5SF \\ 98.75SF + 3072 \\ 146.75SF \end{array}$
64 bits/symbol	$ \begin{array}{l} {\rm DCS\text{-}}M\text{-}{\rm DCSK}(N=10,M=4)\\ {\rm MC\text{-}}CSK\ [10](N=16) \end{array} $	93SF - 74 32SF - 361	$\begin{array}{c} 112SF \\ 32SF \end{array}$

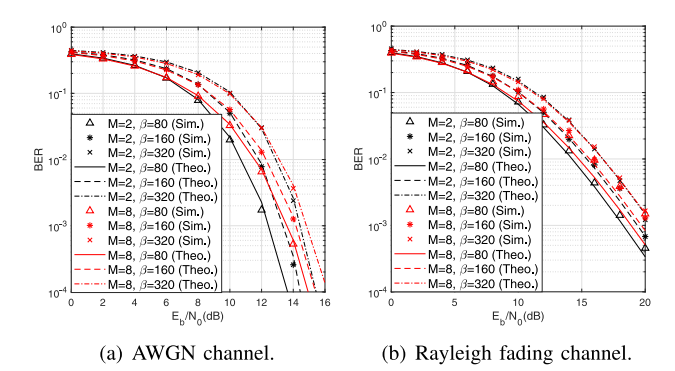


Fig. 5. Theoretical and simulated BER performances of the DCS-M-DCSK system with N=8.

are respectively 4, 4, 24 bits/symbol while the bandwidth efficiency is $\frac{4}{SF}$, $\frac{4}{SF}$ and $\frac{24}{SF}$.

It can be observed from Table II that the computational complexity of our proposed scheme is lower than benchmark schemes except the MC-CSK (N=16) system. However, MC-CSK system requires additional modules such as multiplexers to implement multi-carrier transmission, hence has higher implementation complexity than the proposed scheme.

C. PAPR Analysis

The PAPR performance can be evaluated by a complementary cumulative distribution function (CCDF) defined as [14]

$$CCDF(PAPR_0) = Pr(PAPR > PAPR_0)$$
 (14)

where $Pr(PAPR > PAPR_0)$ denotes the probability that PAPR is larger than the average PAPR denoted by $PAPR_0$. Then we can evaluate the PAPR in the k-th symbol duration by $PAPR = \frac{max(|S^k|^2)}{E(|S^k|^2)}$, where $max(\cdot)$ represents the maximization operation to obtain the maximum value of (\cdot) .

IV. SIMULATION RESULTS

In this section, we present simulated results. In our simulations, the definitions of system parameters have been presented in Section III-B. Besides, the parameters of multipath Rayleigh fading channel are set as $E[\alpha_1^2] = E[\alpha_2^2] = E[\alpha_3^2] = 1/3$, $\tau_1 = 0$, $\tau_2 = 5T_c$, $\tau_3 = 20T_c$ for large delay spreading and $\tau_1 = 0$, $\tau_2 = 2T_c$, $\tau_3 = 5T_c$ for small delay spreading, where for the *i*-th path, α_i represents the channel coefficient and τ_i is the time delay.

A. BER Performance

Fig. 5(a) and Fig. 5(b) illustrate the simulated (Sim.) and theoretical (Theo.) BER results of the DCS-M-DCSK system with different M and β over the AWGN channel and the small-delay-spreading multipath Rayleigh fading channel respectively. It can be observed that when β is larger, the theoretical BER results will match simulated ones better thanks to higher Gaussian approximation precision. Moreover,

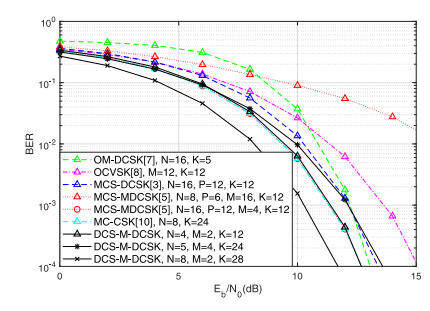


Fig. 6. BER performance comparisons over AWGN channel with SF = 80.

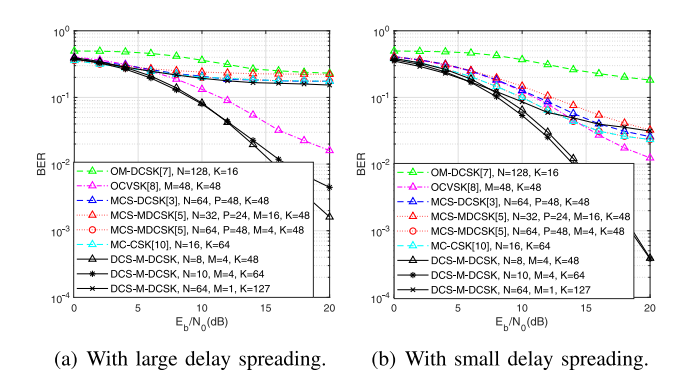


Fig. 7. BER performance comparisons over multipath Rayleigh fading channel with SF=640.

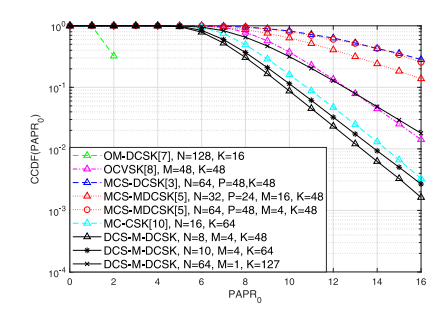


Fig. 8. CCDF PAPR performance comparisons with SF = 640.

when M and β decrease, the interferences between signals will reduce accordingly, which leads to better BER performances.

Furthermore, Fig. 6 and Fig. 7 compare the BER performances of the proposed DCS-M-DCSK and benchmark schemes including OM-DCSK [7], MCS-DCSK [3], MCS-MDCSK [5], MC-CSK [10] and OCVSK [8] over the AWGN channel when SF = 80 and multipath Rayleigh fading channel with large or small delay spreading when SF = 640. It can be seen from Fig. 6 that for the same $SF = N\beta$, when N is larger, β will be smaller, the noises decrease as given in Eq. (9) and the BER performances of the proposed system are improved accordingly. Additionally, we can notice that when N increases to 8, the proposed system can provide better BER performances than those of benchmark schemes using N = 8, 16, while achieving much higher data rate K = 28.

In Fig. 7, for the multipath Rayleigh fading channel with large delay spreading or small delay spreading, we can notice that the proposed DCS-*M*-DCSK system outperforms benchmark schemes and achieves better BER performances at the same data rate *K*. Thus, thanks to the DCS design, the proposed scheme can better combat the multipath interferences [1] and is more robust to channel variations.

B. PAPR Performance

At last, Fig. 8 shows that the PAPR performances of the DCS-M-DCSK system are lower than counterpart schemes except the OM-DCSK scheme which can not provide high data rate transmissions. Moreover, with higher data rate of K = 127, the PAPR performances of our design are also better than those of MCS-DCSK and MCS-MDCSK systems.

V. CONCLUSION

In this brief, we propose a high data rate DCS-M-DCSK scheme with low PAPR. In our design, multiple orthogonal chaotic basis vectors are constructed to modulate the user data bits as reference vectors, then the discrete cosine codes are utilized to spread the information-bearing chaotic modulated vectors for transmissions over the quadrature and inphase channels. Theoretical BER expressions are derived, and the data rate as well as the computational complexity is analyzed and compared among benchmark schemes. Simulation results validate our derivations. Moreover, the results demonstrate the proposed design can achieve better BER performances than benchmark schemes over multipath fading channels with the same data rate and lower PAPR. Therefore, the proposed DCS-M-DCSK system can provide higher data rate services for user ends with the improved bandwidth efficiency, better robustness over multipath fading channels, and lower PAPR.

REFERENCES

- W. K. Xu, L. Wang, and G. Kolumbán, "A novel differential chaos shift keying modulation scheme," *Int. J. Bifurcation Chaos*, vol. 21, no. 3, pp. 799–814, 2011.
- [2] W. K. Xu, L. Wang, and G. Kolumbán, "A new data rate adaption communications scheme for code-shifted differential chaos shift keying modulation," *Int. J. Bifurcation Chaos*, vol. 22, no. 8, pp. 1–8, 2012.
- [3] T. Huang, L. Wang, W. Xu, and F. C. M. Lau, "Multilevel code-shifted differential-chaos-shift-keying system," *IET Commun.*, vol. 10, no. 10, pp. 1189–1195, 2016.
- [4] Y. Tan, W. Xu, and S. Hong, "An M-ary code shifted differential chaos shift keying scheme," in Proc. 23rd Asia–Pac. Conf. Commun. (APCC), Perth, WA, Australia, Dec. 2017, pp. 1–6.
- [5] X. Cai, W. Xu, R. Zhang, and L. Wang, "A multilevel code shifted differential chaos shift keying system with M-ary modulation," IEEE Trans. Circuits Syst. II, Exp. Briefs, vol. 66, no. 8, pp. 1451–1455, Aug. 2019.
- [6] Z. Galias and G. M. Maggio, "Quadrature chaos-shift keying: Theory and performance analysis," *IEEE Trans. Circuits Syst. I, Fundam. Theory Appl.*, vol. 48, no. 12, pp. 1510–1519, Dec. 2001.
- [7] H. Yang, W. K. S. Tang, G. Chen, and G.-P. Jiang, "System design and performance analysis of orthogonal multi-level differential chaos shift keying modulation scheme," *IEEE Trans. Circuits Syst. I, Reg. Papers*, vol. 63, no. 1, pp. 146–156, Jan. 2016.
- [8] T. J. Wren and T. C. Yang, "Orthogonal chaotic vector shift keying in digital communications," *IET Commun.*, vol. 4, no. 6, pp. 739–753, Apr. 2010.
- [9] F. S. Hasan and A. A. Valenzuela, "Design and analysis of an OFDM-based orthogonal chaotic vector shift keying communication system," *IEEE Access*, vol. 6, pp. 46322–46333, 2018.
- [10] H. Yang, W. K. S. Tang, G. Chen, and G.-P. Jiang, "Multi-carrier chaos shift keying: System design and performance analysis," *IEEE Trans. Circuits Syst. I, Reg. Papers*, vol. 64, no. 8, pp. 2182–2194, Aug. 2017.
- [11] S. J. Cox, "Gram-schmidt orthogonalization," in Encyclopedia of Statis-Tical Sciences. Atlanta, GA, USA: American Cancer Soc., 2006.
- [12] Z. D. Wang and B. Hunt, "The discrete cosine transform—a new version," in *Proc. IEEE Int. Conf. Acoust. Speech Signal Process. (ICASSP)*, vol. 8. Boston, MA, USA, Apr. 1983, pp. 1256–1259.
- [13] N. Ahmed, T. Natarajan, and K. R. Rao, "Discrete cosine transform," IEEE Trans. Comput., vol. C-23, no. 1, pp. 90–93, Jan. 1974.
- [14] T. Huang, L. Wang, W. Xu, and G. Chen, "A multi-carrier M-ary differential chaos shift keying system with low PAPR," *IEEE Access*, vol. 5, pp. 18793–18803, 2017.